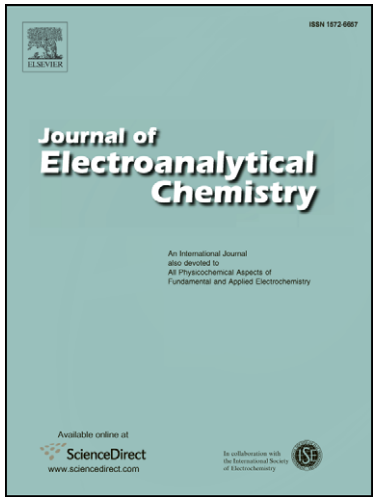

Gold electrodeposition in organic media

Lorena M.A. Monzon, Fiona Byrne, J.M.D. Coey

PII: S1572-6657(11)00132-9
DOI: 10.1016/j.jelechem.2011.03.010
Reference: JEAC 459

To appear in: *Journal of Electroanalytical Chemistry*

Received Date: 7 December 2010
Revised Date: 7 March 2011
Accepted Date: 10 March 2011

Please cite this article as: L.M.A. Monzon, F. Byrne, J.M.D. Coey, Gold electrodeposition in organic media, *Journal of Electroanalytical Chemistry* (2011), doi: 10.1016/j.jelechem.2011.03.010

Gold electrodeposition in organic media

Lorena M. A. Monzon*, Fiona Byrne and J. M. D. Coey

School of Physics, Trinity College Dublin, Ireland

*aranzazl@tcd.ie

Abstract

Organic species are easily adsorbed onto metal electrodes, due to the high surface energy. This principle is widely employed in electrodeposition to obtain grains with a given shape and size. Electrodeposition in organic electrolytes and ionic liquids is expected to produce deposits whose properties will be modified by the nature of the species present in the bath. Here, we analyse the voltammetric profiles for the reduction of two different gold complexes, tetrachloroaurate (III) ($AuCl_4^-$) and dicyanoaurate (I) ($Au(CN)_2^-$), in dimethylsufoxide (DMSO) and in the ionic liquid tributylmethylammonium bis(trifluoromethylsulfonyl)imide ($TBMA^+NTf_2^-$). We evaluate how organic cations present in the electrolyte modify not only the voltammetric response but also the morphology of the deposits obtained. The films range from very smooth with a rms roughness of ~ 10 nm for 500 nm film to rough globular or facetted films with a crystalline size of ~ 200 nm.

Keywords

tetrabutylammonium, shape-control agent, SEM, AFM, voltammetry, kinetic constant.

1. Introduction

The electrodeposition of highly electropositive metals is performed in electrolytic baths where high voltages are accessible. At present, materials such as Al, La, Ta, Ga, Na and Si, among others, are deposited in organic electrolytes or ionic liquids where the chemical stability of the organic species leads to a wider potential window.[1-6]

Capping agents are used in electrodeposition to guide the growth of metal or semiconductor crystals.[7-19] These organic species adsorb onto electrodes and electrodeposits as a result of the high surface energy of these materials, which ultimately influence the shape of the growing grains. Therefore, the chemical nature of the organic ions present in ionic liquids and organic electrolytes may have a strong impact on the morphology of the deposits produced. To address this, we chose to electrodeposit a noble metal, gold, because the films obtained remain stable after exposure to air, allowing the morphology to be readily characterised.

We analyse the cyclic voltammograms of $AuCl_4^-$ and $Au(CN)_2^-$ in dimethylsulfoxide (DMSO) containing different electrolytes. The adsorption of tetrabutylammonium (TBA^+) onto the electrode surface is evaluated through the electrochemical characterisation of the reduction of $AuCl_4^-$. The voltammetric profiles are correlated with the SEM images of the films. Images of deposits grown in the ionic liquid tributylmethylammonium bis(trifluoromethylsulfonyl)imide ($TBMA^+NTf_2^-$) are included for comparison. Although the electro-reduction of $AuCl_4^-$ in organic media has been reported,[20-23] the physicochemical aspects of the differences with its reduction in water were not discussed. Here, we analyse the thermodynamic aspects involved during this process and their implications.

2. Experimental

Electrochemical measurements were carried out in a Braun 130 glovebox with O_2 level < 1 ppm and H_2O 3-4 ppm using a CHI 660 potentiostat, with iR drop compensation. A three-electrode arrangement was used. A gold disk 5mm diameter was employed as the working electrode and platinum mesh as the counter electrode. The reference electrode was a commercial silver wire in a capillary tube immersed in the supporting electrolyte solution employed and separated from the analyte solution by a porous frit. After each experiment, a ferrocene solution was added as an internal standard to set the potential scale. The working electrode was polished prior to every experiment with 1 μm, 0.3 μm and 0.05 μm alumina slurries on lapping pads, followed by electrochemical cleaning in a 0.2 M H_2SO_4 solution purged with Argon: potential pulses of 2 seconds at 2V and -2V vs. Ag/AgCl/0.1M Cl^- were applied during 1 minute. The electrode was rinsed with deionised water, carefully dried with N_2 and transported into the glovebox.

Dimethylsulfoxide (DMSO) anhydrous was dried with activated molecular sieves, 4 Å (Sigma). The molecular sieves were activated in a furnace at 350ºC during 1 day and added to the DMSO. The solvent was allowed to dry for one week and stored in the glovebox. The supporting electrolytes employed were tetrabutylammonium (TBA^+) or potassium perchlorate (Sigma). They were dried at 70ºC under vacuum. Anhydrous potassium tetrachloroaurate (III) and potassium dicyanoaurate (I) were obtained from Sigma and opened, weighted and always kept in a dried atmosphere. $TBMA^+NTf_2^-$ ionic liquid was prepared via metathesis of tributylmethylammonium chloride and lithium bis(trifluoromethylsulfonyl)imide, in water. Gold salts soluble in the ionic liquid were synthesised in a similar fashion. An aqueous solution of tributylmethylammonium chloride was added to an aqueous

solution of potassium tetrachloroaurate (III) or potassium dicyanoaurate (I) to produce ($TBMA^+AuCl_4^-$) or ($TBMA^+Au(CN)_2^-$) respectively. $TBMA^+AuCl_4^-$ precipitate as a yellow solid and ($TBMA^+Au(CN)_2^-$) separates from the aqueous solution as an oily phase. $TBMA^+AuCl_4^-$ was purified by recrystallization and dried at 80^0C. $TBMA^+Au(CN)_2^-$ and $TBMA^+NTf_2^-$ were washed with water several times and dried under vacuum at 80^0C overnight. For SEM images, the films were grown potentiodynamically, on gold substrates with an exposed area of 1.13 cm^2. The Au/Si(100) subtrates were prepared by e-beam evaporation of 20 nm of chromium followed by 100 nm of gold using a BOC Edwards Auto 500 evaporator (base pressure: 5 10^{-7} mbar). Prior each electrodeposition, they were cleaned with H_2O_2 + 1 M KOH, followed by electrochemical stripping in 1 M KOH.[24] The clean substrates were blown with N_2 and transported into the glovebox. Voltammetric simulations were carried out, employing the Windows-based software supplied with the 660 CHI potentiostat.

The surface topography and roughness (rms) of some of the resulting films were also determined using an Asylum MFP-3D atomic force microscope (AFM). Morphology and composition were studied by scanning electron microscopy (SEM) and energy dispersive x-ray analysis (EDAX).

3. Results and discussion

3.1 Electrochemistry of $AuCl_4^-$

In aqueous solutions, the reduction of $AuCl_4^-$ to metallic gold takes place via a single three-electron process, [25-27]. $AuCl_2^-$ does not appear as an intermediate in aqueous solutions because its formation is less favourable (the standard redox potential for the reduction of $AuCl_4^-$ to metallic gold is larger than to $AuCl_2^-$).

$$AuCl_{4\,(aq)}^{-} + 3\,e^{-} \rightarrow Au_{(s)} + 4\,Cl_{(aq)}^{-} \qquad E^{0} = \ 1.002\,V\ vs\ NHE \qquad (1)$$

$$AuCl_{4\,(aq)}^{-} + 2\,e^{-} \rightarrow AuCl_{2\,(aq)}^{-} + 2\,Cl_{(aq)}^{-} \qquad E^{0} = \ 0.926\,V\ vs\ NHE \qquad (2)$$

In organic solvents [20,21] and ionic liquids [22,23], on the other hand, this reduction occurs in two consecutive electrochemical steps, at two different potentials:

$$AuCl_{4\,(o)}^{-} + 2\,e^{-} \rightarrow \ AuCl_{2\,(o)}^{-} + 2\,Cl^{-} \qquad E_1 \qquad (3)$$

$$AuCl_{2\,(o)}^{-} + \ e^{-} \rightarrow \ \ Au_{(s)} + 2\,Cl^{-} \qquad E_2 \qquad (4)$$

To the best of our knowledge, no physicochemical explanation has been given for this difference. We think that a possible reason might be the poor solvation of Cl^- ions in aprotic solvents and ionic liquids. It is accepted that the solubility of small anions is determined by the electron pair acceptability of the solvent, which in the case of DMSO is 19.3 against 54.8 for water.[28] Therefore, the solvation of DMSO towards halide ions is predicted to be much weaker than it is in water, making the release of four Cl^- in one single step thermodynamically unlikely. In the case of ionic liquids, the solubility of halides is mainly determined by supra-molecular interactions with the cation of the ionic liquid. Given the low dielectric constant of ionic liquids, typically ~ 10,[29,30] the ion-pair interactions are strong.[31,32] It has been shown that even small amounts of Cl^- ions dissolved in ionic liquids increase their viscosity dramatically,[33] which reflects the structuring effect exerted by such small hydrophilic ions. This is in agreement with thermodynamic calculations that predict solvation entropies of halides in ionic liquids to be negative.[34] All this evidence indicates that the insertion of Cl^- in ionic liquids or aprotic solvents modifies the solvent environment unfavourably, increasing the energy barrier of the overall electrochemical reaction. A similar behaviour was reported in the electrochemistry of $TiCl_4$ in ionic liquids, where the impossibility of electrodepositing Ti was attributed to 'kinetics and thermodynamic barriers' imposed by the media.[35]

Fig. 1 shows cyclic voltammograms of $AuCl_4^-$ in DMSO. In the figure, P_1 and P_2 correspond to the reactions (3) and (4), respectively. Each cycle shown in the figure is the first scan recorded in separated experiments, after the surface of the electrode was previously polished. It can be noted that after the surface has been polished the formation of the intermediate in solution, P_1, is reproducible. On the contrary, the formation of metallic gold, P_2, is not. This fact indicates that the electroreduction of $AuCl_2^-$ to metallic gold is highly dependent on the surface morphology of the polycrystalline working electrode. Moreover it has been reported that it also depends on the electrode material.[22] In the reverse scan, the cathodic peak P_3 shows the reactivation of the electrode. In general, this happens when inhibitory species are removed from the surface leaving the electrode exposed again to more gold electrodeposition, at potentials where the electrodeposition of gold is still favourable. Contrary to what one might expect, P_4 has been assigned to the oxidation of Cl^- to Cl_2 rather than to the formation of $AuCl_2^-$ or $AuCl_4^-$, given that similar anodic peaks were recorded with solutions containing only Cl^-, at glassy carbon electrodes.[36] The stripping of gold to produce gold chloride complexes takes place at much larger anodic overpotentials.[21,22] The inset of the figure shows the voltammetric response obtained in the ionic liquid $TBMA^+NTf_2^-$. Although the voltamograms recorded in DMSO and in $TBMA^+NTf_2^-$ are quite similar, the magnitude of the current in the later case is considerably smaller. This is related to the high viscosity of the medium.[37,38]

A detailed analysis of P_1 will allow us to evaluate and quantify the interaction of organic ions with the electrode surface. A series of experiments was carried out in 0.1 M $KClO_4$ or using 0.1 M $TBAClO_4$ as supporting electrolyte. In all cases, peak current I_p^1, and peak potential, E_p^1, values for the reduction of $AuCl_4^-$ to $AuCl_2^-$ were

plotted against the square root of the scan rate, v, and log v, respectively. In Fig. 2a-b are shown the experimental data obtained with $KClO_4$ as supporting electrolyte. In all cases, it was found that the electrochemical reduction of $AuCl_4^-$ to $AuCl_2^-$ is irreversible given that I_p^1 vs $v^{1/2}$ and E_p^1 vs log v are linear.[39] Without organic ions, the slope of E_p^1 vs log v gives a $n'\alpha_c$ value of 0.86 ± 0.04, where n' represents the number of electrons involved in the rate-determining step and α_c the cathodic transfer coefficient. Given that $n'\alpha_c \leq 1$, it is deduced that the number of electrons involved in the kinetic step is one, with α_c = 0.86 ± 0.04.[39] In other words, since the electrochemical step P_1 is a two-electron process, the transfer of one of the two electrons is slow while the other one is fast. The diffusion coefficient (D) of $AuCl_4^-$ in DMSO was calculated from the slope of I_p^1 vs $v^{1/2}$ giving a value of (4.43 ± 0.03) 10^{-6} cm^2 s^{-1}, half of the one reported in water, 9.0 10^{-6} cm^2 s^{-1}.[40] It is known that the diffusion is strongly influenced by the viscosity (η) of the solvent. According to the Stokes-Einstein equation D is inversely proportional to η.[41] Thus, it is deduced that in more viscous solutions the diffusion will be slower. At 25^0C the viscosity of DMSO and water are 1.99 mPa s [42] and 0.89 mPa s [43], respectively, which predicts D_{H_2O} values almost two times larger than D_{DMSO}, in agreement with the value determined here.

The standard kinetic constant (k^0) for the reduction of $AuCl_4^-$ to $AuCl_2^-$ can be calculated from the intercept of a plot of $\ln I_p^1$ vs. (E_p - E^0), which is $\ln(0.227nFAC^{\infty}k^0)$, where E^0 is the standard redox potential, n the total number of electrons involved in the electrochemical reaction, F the Faraday constant, A the area of the electrode and C^{∞} the concentration of $AuCl_4^-$ in the solution.[39] However, since E^0 is not known, the potential where the reaction starts, E_{rxn}, was used instead,[44] as

recommended by Nicholson and Shain.[45] In the absence of organic ions, the k^0 value derived was (1.2 ± 2) 10^{-5} cm s^{-1}. From the slope of the graph, ($n'\alpha_c F/RT$) $n'\alpha_c$ is 0.77 ± 0.03, close to 0.86 ± 0.04 obtained by linear regression of E_p vs log v. Voltammetric simulations like the ones shown in Fig. 2d corroborate the accuracy of the parameters calculated. Details on the way the electrochemical parameters $n'\alpha_c$, k^0 and D are calculated can be found in ref. 44.

The use of bulky organic cations in the supporting electrolyte can lead to interesting changes in the electrochemical profiles and modify the surface morphology of the electrodeposits. Fig. 3 shows the cyclic voltammograms recorded in solutions containing the same $AuCl_4^-$ concentration. Black and red lines were obtained when $KClO_4$ or $TBAClO_4$ were employed as electrolytes. As it can be seen in the figure, TBA^+ causes a marked shift of E_p^1 towards more cathodic potentials, a decrease in the overall current and a less steep increase in the current at low over-potentials. It has been reported that, given its hydrophobicity, TBA^+ modifies the double layer capacity of gold electrodes [46] and for the same reason; it protects titanium against chemical etching.[47] At more cathodic potentials the accumulation of TBA^+ at the surface should increase, modifying in turn nucleation processes. Its interaction with the electrode surface has two effects. First, the decrease in I_p^1 value observed is mainly caused by a reduction of the exposed surface area, which it is estimated by comparison of the slopes of the graphs I_p^1 vs. $v^{1/2}$ for the experiments carried out in $KClO_4$ in DMSO and in $TBAClO_4$ in DMSO. Our results indicate that ~ 34 % of the working electrode is covered by TBA^+ at ~ -0.3 V. Such large coverage of the surface leads to the second observation, the shift in E_p^1, which reflects the hindrance of the electrochemical reduction of $AuCl_4^-$ to $AuCl_2^-$. That is, the partial

adsorption of this large hydrophobic cation slows down the rate of the electron transfer process. It is important to point out that these effects are only significant because the reduction of $AuCl_4^-$ takes place quite below the potential of zero charge, where the adsorption of hydrophobic cations is significant.[48] The k^0 value calculated for the reduction of $AuCl_4^-$ to $AuCl_2^-$ with TBA^+ in the electrolyte was (2.2 ± 1) 10^{-6} cm s^{-1}, around one order of magnitude smaller than in its absence. Simulations were performed employing these electrochemical parameters, leading to a good agreement with the experimental profiles (see inset Fig. 3). It seems that TBA^+ slows down electron transfer reactions but it is only perceptible in already kinetically controlled processes.[49,50] The influence of TBA^+ on the morphology of gold electrodeposits will be discussed in section 3.3.

3.2 Electrochemistry of $Au(CN)_2^-$

Gold was also electrodeposited from organic solutions containing $Au(CN)_2^-$. The electro-reduction of $Au(CN)_2^-$ takes place at more negative potentials than $AuCl_4^-$ because $Au(CN)_2^-$ is very stable. According to several authors, the reduction of $Au(CN)_2^-$ to metallic gold in water follows two different mechanisms. At low overpotentials, $Au(CN)_2^-$ first adsorbs at the surface, and then it reduces to $Au_{(s)}$.[51-54]

$$Au(CN)_{2(w)}^- \rightarrow AuCN_{ad} + CN^- \qquad (5)$$

$$AuCN_{ad} + e^- \rightarrow Au_{(s)} + CN^- \qquad (6)$$

whereas at higher overpotentials the reduction proceeds in one step,

$$Au(CN)_{2(w)}^- + e^- \rightarrow Au_{(s)} + 2\,CN^- \qquad (7)$$

In DMSO, only one cathodic peak is recorded (~ -2.5 V) which suggests at first that the reduction of $Au(CN)_2^-$ follows only one electrochemical path. (See Fig.

4a, red line) The plots of I_p vs $v^{1/2}$ and E_p vs log v are linear which, together with the difference between the anodic and cathodic peaks of ~ 1 V indicates that this reaction is electrochemically irreversible. However, the simulations obtained with the electrochemical parameters derived from plots equivalent to the ones shown in Fig. 2 do not match the experimental profiles (Fig. 4a). At low overpotentials, it can be seen that the current of the experimental curve is larger than the one in the simulation. Besides, on the experimental curve, there are two overlapping anodic peaks on the reversed scan. These profiles were reproducible every time the gold surface is polished, which indicates that these differences cannot be attributed to preferred electrodeposition and growth on different facets. Consequently, the cathodic peak for the reduction of $Au(CN)_2^-$ must be the result of processes (6) and (7) taking place simultaneously. In the ionic liquid $TBMA^+NTf_2^-$, on the other hand, these two reactions take place at slightly more different potentials, since two separated peaks appear overlapped (see inset Fig. 4a). Given that reactions (6) and (7) cannot be studied separately, no reliable electrochemical parameters were derived from these experiments.

As it was noted before in the reduction of $AuCl_4^-$ to $AuCl_2^-$, the voltammograms recorded with TBA^+ in the solution also exhibit a shift of E_p towards more cathodic potentials and a decrease in the overall current (Fig. 4b).

3.3 Morphology of films produced in $AuCl_4^-$ and $Au(CN)_2^-$ and solutions

To analyse the effect of the organic media on gold electrodeposits, films were grown keeping the concentration constant (10 mM) while the electrolyte nature was changed. In Fig. 5 are the SEM images of films produced from $AuCl_4^-$ baths and in Fig. 6 those obtained from $Au(CN)_2^-$ solutions. Each row corresponds to films grown

at the same applied potential: those at the top were deposited in the kinetic-controlled regime, while those at the bottom were produced under diffusion-controlled conditions.

It is well established that the quality and properties of gold electrodeposits is strongly influenced by the nature of the complex employed.[55,56] For instance, in the kinetic-controlled regime, the deposits produced by the reduction of $AuCl_4^-$ (Fig. 5a-c) have uneven grain growth, while the films obtained from $Au(CN)_2^-$ solutions are more uniform (Fig. 6a-c). As it was mentioned earlier, the reduction of $AuCl_2^-$ to metallic gold is strongly dependent on surface morphology of the electrode, given that P_2 is not reproducible after the electrode has been polished (See Fig. 1). This together with the in-plane image of the deposits obtained at low overpotentials (Fig. 5a-c) indicates that the local facets present in the substrate lead to a preferential nucleation and growth of certain grains. Baker et. al.[57] have recently shown that the bonding between Cl and the Au(111) surface is primarily covalent while with the other faces remain ionic. Thus, the shielding effect of Cl chemically adsorbed onto Au(111) will produce different growth rates of the crystallite facets. It is worth mentioning that at higher overpotentials, this wide size distribution of the grains is only maintained in the absence of organic cation species (compare left column in Fig. 5 with the middle and right columns in the same figure).

Left, middle and right columns in Fig. 5 and 6 are the images of deposits produced in solutions containing K^+, TBA^+ and $TBMA^+$, respectively. In Section 3.1 it was estimated that TBA^+ present in the electrolyte covers at least 34% of the electrode surface. Therefore, the electrodeposits formed will preferentially grow on the bare areas of the electrode. In the Figures, this is seen as an increase in roughness. There is also a change in the grain shape. The almost planar cross–like conformation

of TBA^+ [58,59] leads to the formation of star-shape lamellae or rosette deposits (Fig. 5b, e and g; and Fig. 6b and e). The right column of Fig. 5 and 6 are the images for deposits produced when $TBMA^+$ is in the electrolyte. $TBMA^+$ is similar to TBA^+ but with one of its four chains shorter, which resembles a T-shape.[60] When the deposits are obtained from the reduction of $AuCl_4^-$, the gold particles formed seem to be polyhedral rather than spherical (Fig. 5c). When the electrodeposition is carried out in solutions containing $Au(CN)_2^-$, small rectangular grains can be distinguished (Fig. 6c). These polyhedral features could be caused by the particular T-shape of $TBMA^+$ adsorbed at the electrode surface, although the high viscosity of the ionic liquid could favour selectivity towards the formation of crystalline structures.[61,62] The deposits shown at the bottom row in Fig. 6 are produced at potentials where the organic species present in the electrolyte are being reduced as well. They are fibrous sponge-like films.

The roughening effect of TBA^+ was evaluated by AFM. The smoothest films produced are those from $Au(CN)_2^-$ in DMSO, grown under the kinetic-controlled regime. The reproducibility of the voltammogram after polishing the electrode (section 3.2) seems to indicate that the deposition is not influenced by the surface morphology, which could be the reason why these deposits are quite smooth (rms roughness obtained for these films is ~10 nm for a film thickness of ~ 0.5 μm. Film thicknesses were obtained by Faraday's law). Fig. 7a shows a (1 μm x 1 μm) section of this type of deposits. By contrast, the same deposition carried out in the presence of TBA^+ produces rougher films with a rms roughness of ~ 70 nm.

4. Conclusions

The electrodeposition of gold in several organic media was explored. Analysis of the voltammetric profiles and SEM images of the films obtained in the different electrolytes allowed us to understand the role of organic ions on the kinetics and morphology of the deposits produced.

The differences found between the electrochemical reduction of $AuCl_4^-$ in water and DMSO and ionic liquids were explained in terms of the solvation entropy of the released Cl^- anions and weak electron pair acceptability of the media.

The adsorption of TBA^+ at the electrode surface was shown to cover at least 34 % of the total surface area. A decrease of one order of magnitude in the kinetic constant for the reduction of $AuCl_4^-$ to $AuCl_2^-$ was calculated.

Organic ions strongly influence the shape of grains and roughness of gold electrodeposits. This is a key fact to take into account when employing organic media for electrodeposition.

Since electro-catalysis is highly dependent on the presence of active surface states and the morphology of the deposits, some of the baths presented here could be employed to grow rough electrodes for electro-catalytic applications, such as in fuel cells.[63,64]

Acknowledgments

This work was supported by Science Foundation Ireland as part of the MANSE project 05/IN/1850 and on contract RFP OD/RFP/PHY2372. This work was also supported by the FP7 NAMDIATREAM project.

References

[1] E. M. Moustafa, S. Zein El Abedin, A. Shkurankov, E. Zschippang, A.Y. Saad, A. Bund, F. Endres, J. Phys. Chem. B, 111 (2007) 4693-4704.

[2] S. Legeai, S. Diliberto, N. Stein, C. Boulanger, J. Estager, N. Papaiconomou, M. Draye, Electrochem. Comm., 10 (2008) 1661-1664.

[3] L. H. S. Gasparotto, N. Borisenko, O. Höfft, R. Al-Salman, W. Maus-Friedrichs, N. Bocchi, S. Zein El Abedin, F. Endres, Electrochim. Acta, 55 (2009) 218-226.

[4] T. Munisamy, A.J. Bard, Electrochim. Acta, 55 (2010) 3797-3803.

[5] R. Wibowo, L. Aldous, E. I. Rogers, S. E. Ward Jones, R. G. Compton, J. Phys. Chem. C, 114 (2010) 3618-3626.

[6] A. Ispas, B. Adolphi, A. Bund, F. Endres, Phys. Chem. Chem. Phys., 12 (2010) 1793-1803.

[7] Y. Guo, Q. Liao, J. Zhang, D. Xu, J. Phys. Chem. B, 109 (2005) 13519-13522.

[8] S. Jiao, F. Sun, Y. Guo, W. Song, J. Zhao, L. Tang, Z. Wang, J. Crystal Growth, 304 (2007) 425-429.

[9] M. Min, C. Kim, Y.I. Yang, J. Yi, H. Lee, Phys. Chem. Chem. Phys., 11 (2009) 9759-9765.

[10] L. Xu, L. Xu, K. Hu, J. Li, S. Gao, D Xu, J. Phys. Chem. C, 114 (2010) 269-273.

[11] H. Sato, T. Homma, H. Kudo, T. Izumi, T. Osaka, S. Shoji, J. Electroanal. Chem. 584 (2005) 28–33.

[12] M. A. Pasquale, L. M. Gassa, A. J. Arvia, Electrochim. Acta, 53 (2008) 5891-5904.

[13] G. Wei, H. Ge, X. Zhu, Q. Wu, J. Yu, B. Wang, Appl. Surf. Sci., 253 (2007) 7461-7466.

[14] A. Dolati, A. Afshar, H. Ghasemi, Mater. Chem. Phys., 94 (2005) 23-28.

[15] L. Liao, W. Liu, X. Xiao, J. Electroanal. Chem. 566 (2004) 341–350.

[16] J. H. Yang, J. C. Lin, T. K. Chang, X. B. You, S. B. Jiang, J. Micromech. Microeng., 19 (2009) 025015 (1-12).

[17] A. M. Rashidi, A. Amadeh, Surf. Coat. Technol., 204 (2009) 353-358.

[18] A. L. Portela, G. I. Lacconi, M. López Teijelo, J. Electroanal. Chem., 495 (2001)169-172.

[19] R. Fukui,Y. Katayama, T. Miura, Electrochim. Acta, 58 (2011) 1196.

[20] A. D. Goolsby, D. T. Sawyer, Anal. Chem., 40 (1968) 1978-1983.

[21] U. Koelle, A. Laguna, Inor. Chim. Acta, 290 (1999) 44-50.

[22] L. Aldous, D. S. Silvester, C. Villagran, W. R. Pitner, R. G. Compton, M. C. Lagunas, C. Hardacre, New J. Chem, 30 (2006) 1576-1583.

[23] L. Aldous, D. S. Silvester, W. R. Pitner, R. G. Compton, M. C. Lagunas, C. Hardacre, J. Phys. Chem. C, 111 (2007) 8496-8503.

[24] L. M. Fisher, M. Tenje, A. R. Heiskanen, N. Masuda, J. Castillo, A. Bentien, J, Emneus, M. H. Jakobsen, A. Boisen, J. Microel. Eng., 86 (2009) 1282-1285.

[25] K. B. Holt, G. Sabin, R. G. Compton, J. S. Foord, F. Marken, Electroanalysis, 14 (2002) 797-803.

[26] O. M. Magnussen, K. Krug, A. H. Ayyad, J. Stettner, Electrochim. Acta, 53 (2008) 3449-3458.

[27] L. Komsiyska, G. Staikov, Electrochim. Acta, 54 (2008) 168-172.

[28] K. Wakabayashi, Y. Maeda, K. Ozutsumi, H. Ohtaki, J. Molec. Liq., 110 (2004) 43-50.

[29] G. Sese, E. Guardia, J. A. Padro, J. Phys. Chem., 99 (1995) 12647-12654.

[30] N. Sieffert, G. Wiff, J. Phys. Chem. B, 111 (2007) 7253-7266.

[31] H. Weingartner, A. Oleinikova, C. Wakai, C. Daguenet, P. J. Dyson, I. Krossing, J. M. Slattery, J. Phys. Chem. B, 110 (2006) 12682-12688.

[32] I. Krossing, J. M. Slattery, C. Daguenet, P. J. Dyson, A. Oleinikova, H. Weingartner, J. Am. Chem. Soc., 128 (2006) 13427-13434.

[33] K. R. Seddon, A. Stark, M. J. Torres, Pure Appl. Chem., 72 (2000) 2275-2287.

[34] S. Bruzzone, M. Malvaldi, C. Chiappe, J. Chem. Phys., 129 (2008) 074509 (1-9).

[35] F. Endres, S. Zein El Abedin, A. Y. Saad, E. M. Moustafa, N. Borissenko, W. E. Price, G. G. Wallace, D. R. MacFarlane, P. J. Newmanc, A. Bundd, Phys. Chem. Chem. Phys., 10 (2008) 2189–2199.

[36] C. Villagran, C. E. Banks, C. Hardacre, R. G. Compton, Anal. Chem., 76 (2004) 1998-2003.

[37] M. C. Buzzeo, C. Hardacre, R. G. Compton, Anal. Chem., 76 (2004) 4583-4588.

[38] S. R. Belding, E. I. Rogers, R. G. Compton, J. Phys. Chem. C, 113 (2009) 4202-4207.

[39] C. M. A. Brett, A. M. Oliveira Brett in Electrochemistry. Principles, Methods and Applications, Oxford University Press, 2000, pp. 179-182.

[40] H. Martın, P. Carro, A. Hernandez Creus, S. Gonzalez, R. C. Salvarezza, A. J. Arvia, Langmuir 13 (1997) 100-110.

[41] N. G. Tsierkezos, J Solution Chem, 36 (2007), 289-302.

[42] E. W. Flick, Handbook of industrial solvents, 5th edition, Noyres Data Corporation, New Jersey, 1998;

[43] R. C. Weast, *Handbook of Chemistry and Physics*, 53rd, The Chemical Rubber Co, Ohio, 1972.

[44] L. M. A. Monzón, J. Electroanal. Chem., 648 (2010), 47-53.

[45] R. S. Nicholson, I. Shain, Anal. Chem. 36 (1964) 706-723.

[46] A. Tymosiak-Zielinska, Z. Borkowska, Electrochim Acta, 46 (2000) 3073-3082.

[47] K. Shankar, G. K. Mor, A. Fitzgerald, C. A. Grimes, J Phys. Chem. C, 111 (2007) 21-26.

[48] N. Serizawa, Y. Katayama, T. Miura, Electrochim. Acta, 56 (2010) 346–351.

[49] T. Nishiumi, Y. Chimoto, Y. Hagiwara, M. Higuchi, K. Yamamoto, Macromolecules, 37 (2004) 2661-2664.

[50] L. Pospisil, M. Hromadova, R. Sokolova, J. Bulickova, N. Fanelli, Electrochim. Acta, 53 (2008) 4852-4858.

[51] J. A. Harrison, J. Thompson, J. Electroanal. Chem., 40 (1972) 133-142.

[52] B. Bozzini, B.J. Hwang, R. Santhanam, Y.L. Lin, Electroanalysis, 15 (2003) 1667-1676;

[53] B. Bozzini, G. P. De Gaudenzi, C. Mele, J. Electroanal. Chem., 563 (2004) 133-143.

[54] B. Bozzini, C. Mele, V. Romanello, J. Electroanal. Chem., 592 (2006) 25-30.

[55] M. Kato, Y. Okinaka, Gold Bull., 37 (2004) 37-44.

[56] T. A. Green, Gold Bull., 40 (2007) 105-114.

[57] T. A. Baker, C. M. Friend, E. Kaxiras, J. Am. Chem. Soc., 130 (2008) 3720-3721.

[58] J. Lipkowski, V. Y. Komarov, T. V. Rodionova, Y. A. Dyadinb, L. S. Aladkob, J. Supramol. Chem., 2 (2002) 435-439.

[59] P. D. C. Dietzela, M. Jansenb, Z. Anorg. Allg. Chem., 632 (2006) 2276-2280.

[60] S. Katsuta, H. Wakabayashi, M. Tamaru, Y. Kudo, Y. Takeda, J Sol. Chem, 36 (2007) 531-547.

[61] N. Tachikawa, N. Serizawa, Y. Katayama, T. Miura, Electrochim. Acta 53 (2008) 6530–6534.

[62] C. Zhao, D. R. MacFarlane, A. M. Bond, J. Am. Chem. Soc. 131 (2009) 16195–16205.

[63] D. Cameron, R. Holliday, D. Thompson, J. Power Sources, 118 (2003) 298-303.

[64] A. P. O'Mullane, S. J. Ippolito, Y. M. Sabri, V. Bansal, S. K. Bhargava, Langmuir, 25 (2009) 3845-3852.

Fig. Captions

Fig. 1. Cyclic voltammograms for the reduction of $AuCl_4^-$ in DMSO. In the figure are the first cycles recorded in separated experiments. Electrochemical reduction takes place in two steps: at ~ -0.3 V $AuCl_4^-$ reduces to $AuCl_2^-$ (**P_1**) and at ~ -1.1 V $AuCl_2^-$ reduces to $Au_{(0)}$ (**P_2**). Experimental conditions: 5 mM $KAuCl_4$, 0.1 M $KClO_4$, v = 50 mV s^{-1}. Inset: Cyclic voltammogram for the reduction of 5 mM $AuCl_4^-$ recorded in the ionic liquid $TBMA^+NTf_2^-$. v = 50 mV s^{-1}. Working electrode: polycrystalline gold disk electrode, 5 mm diameter.

Fig. 2. **(a)** I_p^1 vs $v^{1/2}$, **(b)** E_p^1 vs log v **(c)** LnI_p^1 vs E_p^1-E_{rxn} **(d)** voltammetric simulation: a two-electron reduction with E_{rxn} = -0.105 V. The rest of the electrochemical parameters are: v = 50 mV s^{-1}, k^0 = 1.1 10^{-5} cm s^{-1}, α_c = 0.8, D = 4.2 10^{-6} cm^2 s^{-1}, [$KAuCl_4$] = 5 mM, A = 0.196 cm^2.

Fig. 3. Effect of the organic supporting electrolyte on the reduction of $AuCl_4^-$. Black and red voltammograms were recorded in DMSO solutions containing 0.1 M $KClO_4$ and 0.1 M $TBAClO_4$, respectively. [$KAuCl_4$] = 5 mM, v = 50 mVs^{-1}. A = 0.196 cm^2.

Inset: The voltammogram recorded in the presence of TBA^+ was simulated with the following electrochemical parameters: a two-electron reduction with E_{rxn} = -0.105 V, v = 50 mV s^{-1}, k^0 = 2.2 10^{-6} cm s^{-1}, α_c = 0.75, D = 4.210^{-6} cm^2, A = 0.13 cm^2.

Fig. 4. Voltammograms for the reduction of $AuCN_2^-$ in DMSO. **(a)** Comparison between a simulation and an experimental profile indicates that the electroreduction of $Au(CN)_2^-$ takes place via more than one electrochemical process. Electrochemical parameters: one electron reduction with E_{rxn} = -1.99 V, v = 100 mV s^{-1}, k^0 = 1 10^{-6} cm s^{-1}, α_c = 0.5, D = 7.1 10^{-6} cm^2 s^{-1}, [$KAu(CN)_2$] = 9 mM, A = 0.196 cm^2. The inset is the voltammogram of $Au(CN)_2^-$ in the ionic liquid $TBMA^+NTf_2^-$. Here, the occurrence of two overlap reductive waves is noticeable. **(b)** Effect of organic supporting electrolyte on the reduction of 9 mM $KAu(CN)_2$. Black and red voltammograms were recorded in DMSO solutions containing 0.1 M $KClO_4$ and 0.1 M $TBAClO_4$, respectively. v = 100 mVs^{-1}.

Polycrystalline gold disk electrode, 5 mm diameter with a geometric area 0.196 cm^2.

Fig. 5. SEM images of films deposited from organic baths containing 10 mM $AuCl_4^-$. Here it is shown how the organic media, together with the potential, modify the morphology of the deposits. Experimental conditions: **left,** 0.1 M $KClO_4$ in DMSO, **middle**, 0.1 M $TBAClO_4$, DMSO and **right**, $TBMA^+NTf_2^-$ ionic liquid. The films were grown potentiodynamically, at **(a-c)** -0.85 V, **(d-f)** -1.00 V and **(g-i)** -1.40 V. Deposited mass 1 mg.

Fig. 6. SEM images of films deposited from organic baths containing 10 mM $Au(CN)_2^-$. The morphology of the deposits depends on the nature of the organic media, as well as the deposition rate. Experimental conditions: **left,** 0.1 M $KClO_4$ in DMSO, **middle**, 0.1 M $TBAClO_4$, DMSO and **right**, $TBMA^+NTf_2^-$ ionic liquid. The films were grown potentiodynamically, at **(a-c)** -2.20 V, **(d-f)** -2.50 V and **(g-i)** -3.00 V. Deposited mass 1 mg.

Fig. 7. The roughening effect of TBA^+ is demonstrated by AFM images. The deposits shown were produced from bath containing 10 mM $Au(CN)_2^-$ in DMSO, with **(a)** $KClO_4$ and **(b)** $TBAClO_4$ as electrolytes. Rms roughness increases from **(a)** 14 ± 2 nm to **(b)** 68 ± 5 nm.

Figure 1

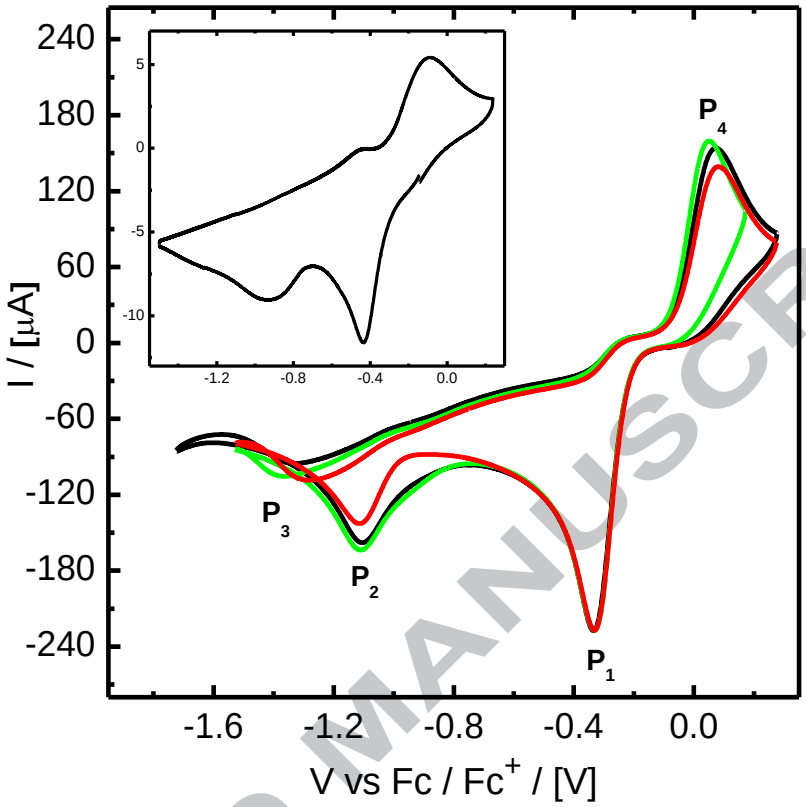

Figure 2

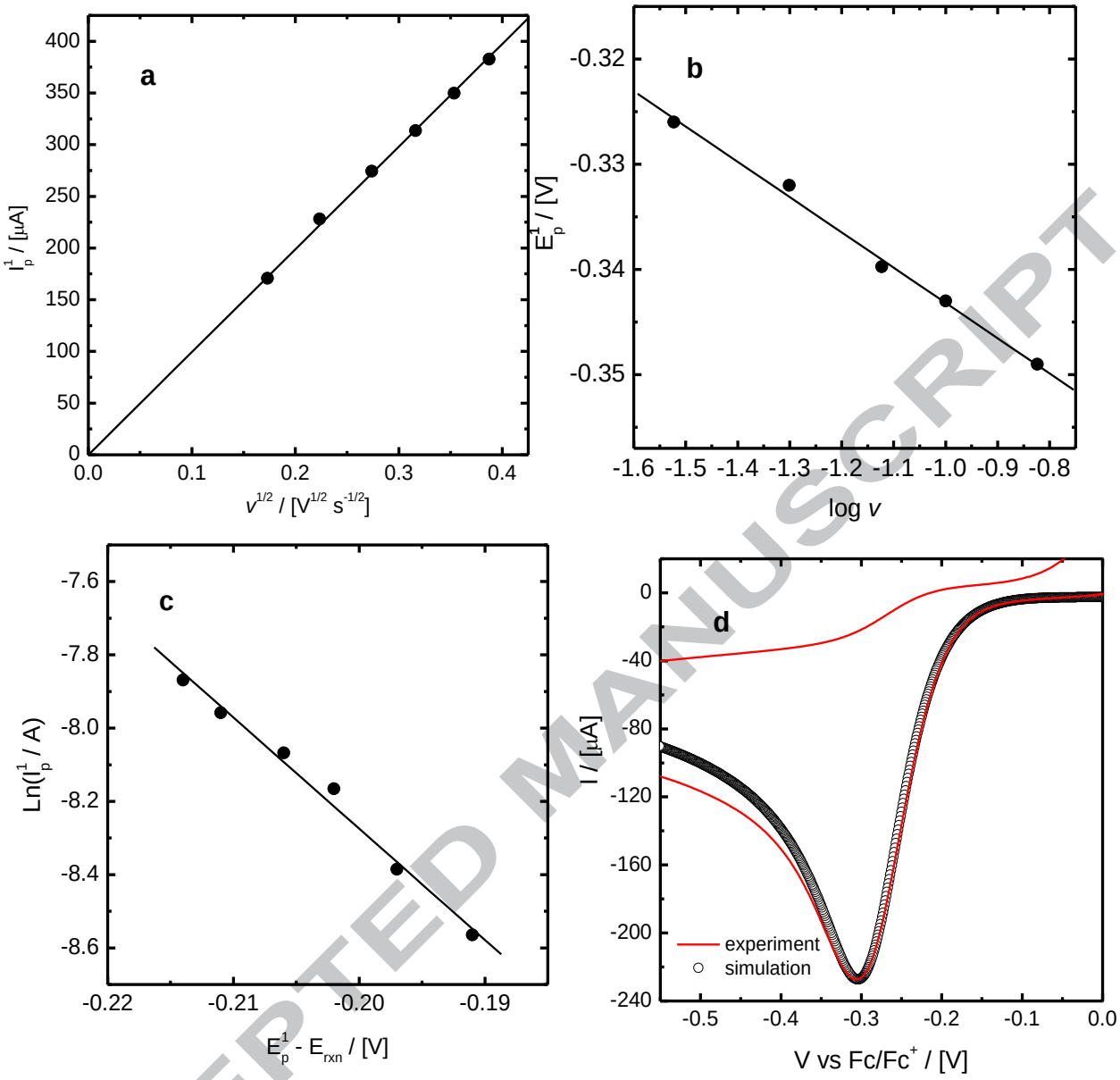

Figure 3

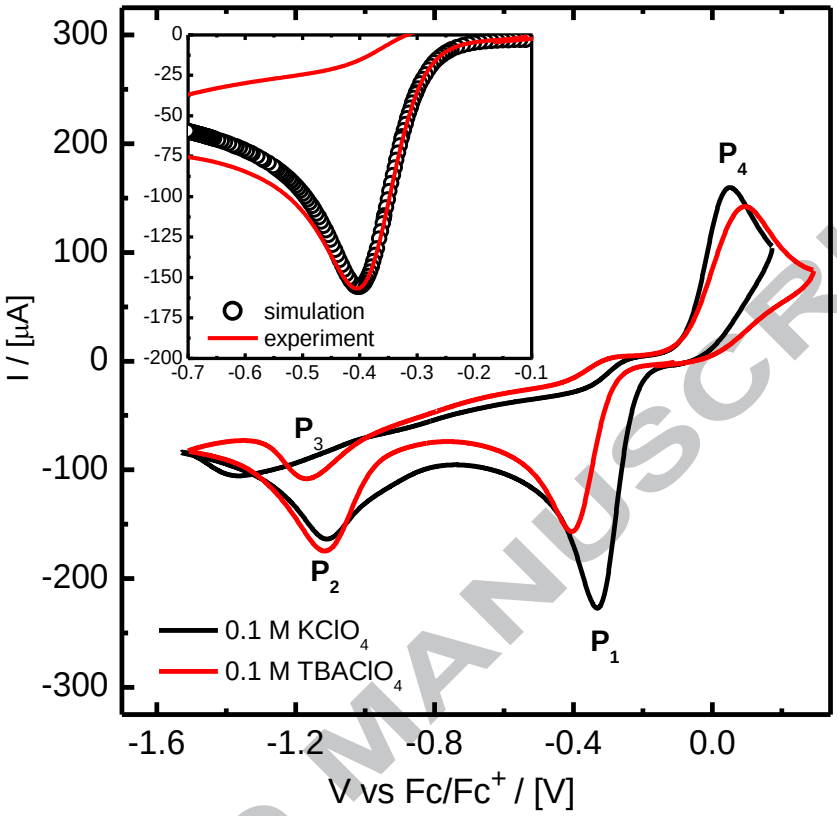

Figure 4

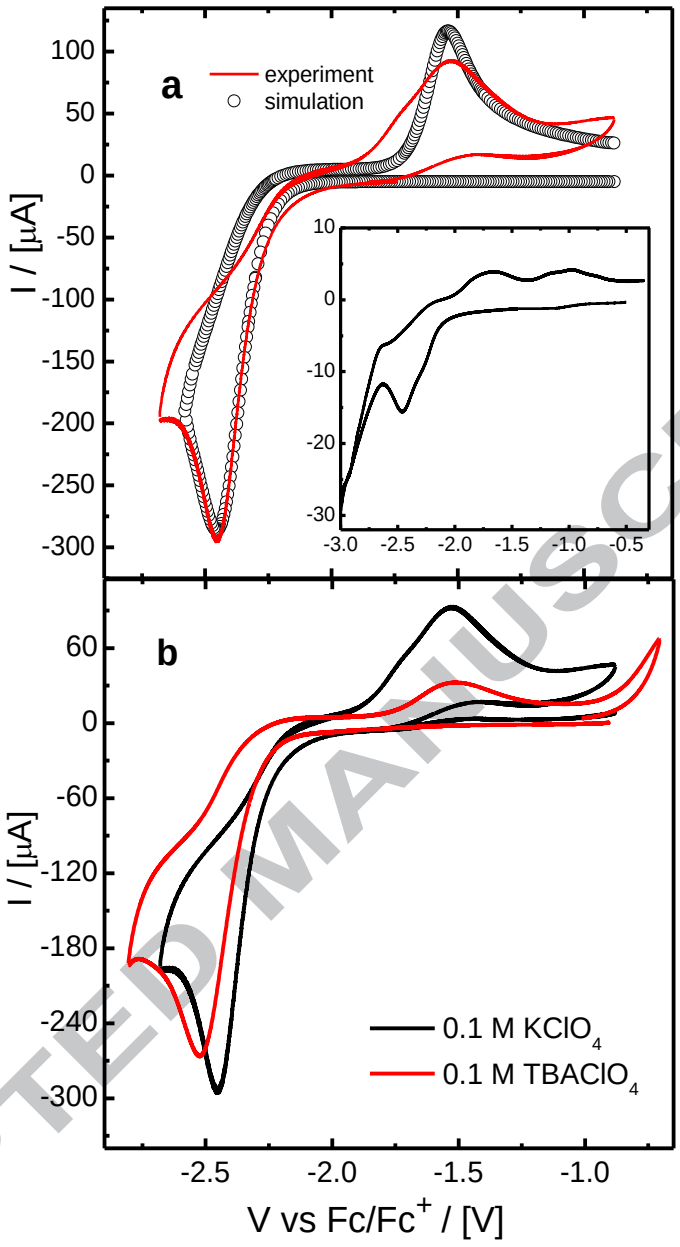

Figure 5

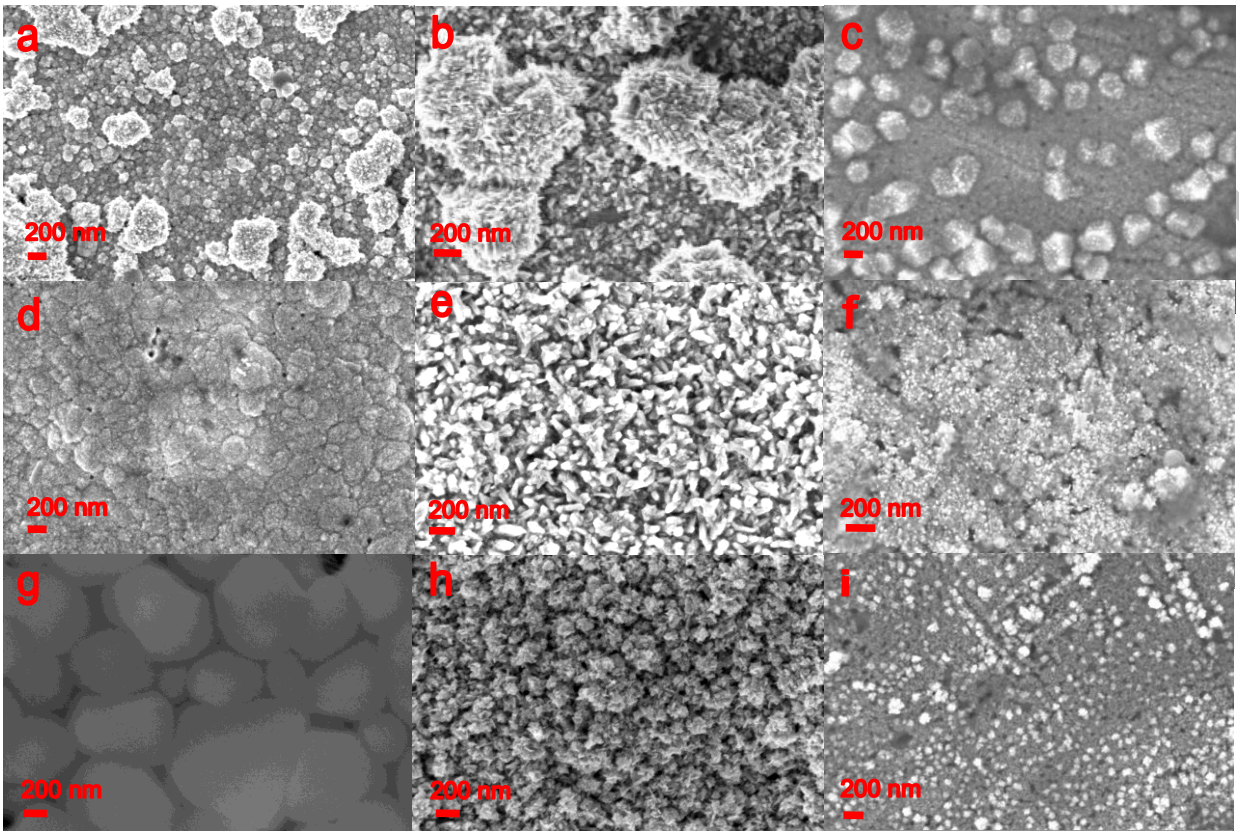

Figure 6

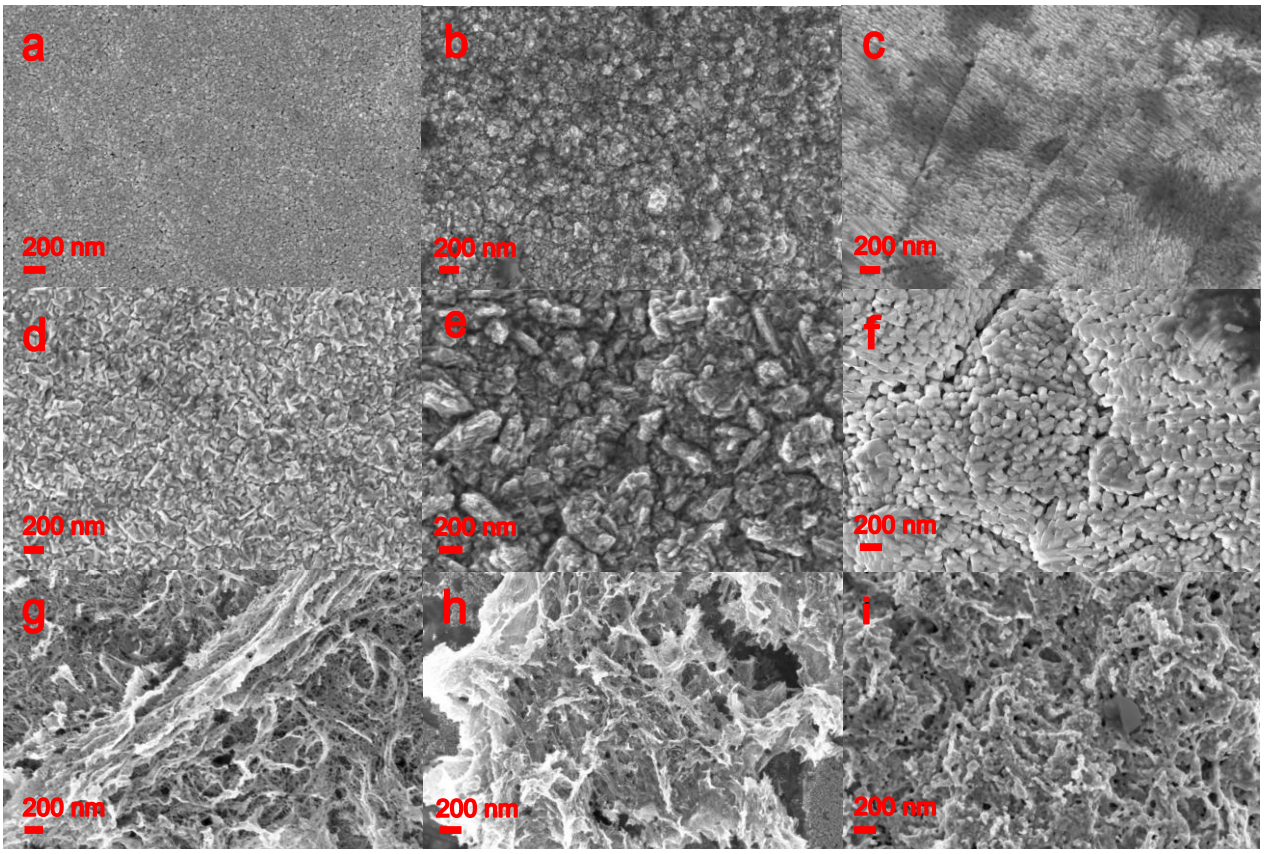

Figure 7

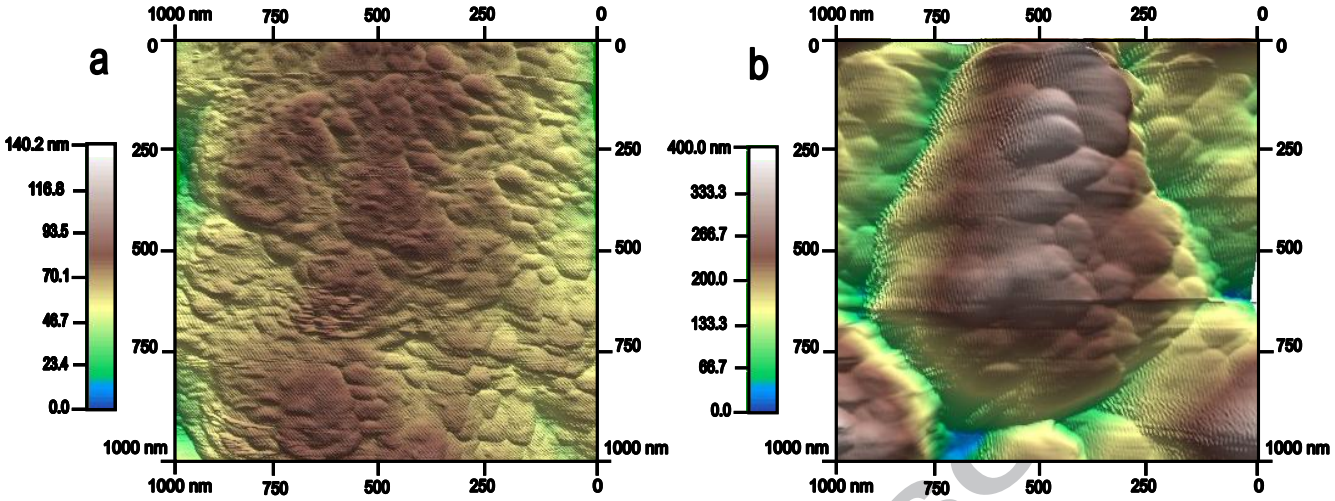

Research Highlights

- The adsorption of Tetrabutylammonium at the electrode surface was shown to cover ~ 30 % of the total surface area.
- A decrease of one order of magnitude in the kinetic constant for the reduction of $AuCl_4^-$ to $AuCl_2^-$ was calculated.
- Organic ions strongly influence the shape of grains and roughness of gold electrodeposits.